

Interaction potential between discrete solitons in waveguide arrays

U. AL KHAWAJA,¹ S. M. AL-MARZOUQ,^{2,3} H. BAHLOULI,^{2,3} AND B. BAIZAKOV⁴

¹Physics Department, United Arab Emirates University, P.O. Box 15551, Al-Ain, United Arab Emirates

²Physics Department, King Fahd University of Petroleum and Minerals, Dhahran 31261, Saudi Arabia

³Saudi Center for Theoretical Physics, Dhahran 31261, Saudi Arabia

⁴Physical-Technical Institute, Uzbek Academy of Sciences, 100084 Tashkent, Uzbekistan

*marzoug@kfupm.edu.sa

Abstract: Using a variational approach, we obtained the interaction potential between two discrete solitons in optical waveguide arrays. The resulting potential bears the two features of soliton-soliton and soliton-waveguide interaction potentials where the former is similar to that of the continuum case and the latter is similar to the effective Pierls-Nabarro potential. The interplay between the two interaction potentials is investigated by studying its effect on the soliton molecule formation. It is found that the two solitons bind if their initial separation equals an odd number of waveguides, while they do not bind if their separation is an even number, which is a consequence of the two solitons being both either at the intersites (unstable) or being onsite (stable). We derived the equations of motion for the solitons' centre of mass and relative separation and provided analytic solutions for some specific cases. Favourable agreement between the analytical and numerical interaction potentials is obtained. Possible applications of our results to all-optical logic gates are pointed out.

© 2016 Optical Society of America

OCIS codes: (190.0190) Nonlinear optics; (000.6800) Theoretical physics; (080.6755) Systems with special symmetry.

References and links

1. V. I. Karpman and V. V. Solov'ev, "A perturbational approach to the two-soliton systems," *Physica D*, **3**,487-502 (1981)
2. J. P. Gordon, "Interaction forces among solitons in optical fibers," *Opt. Lett.* **8**,596-598 (1981)
3. D. Anderson and M. Lisak, "Bandwidth limits due to mutual pulse interaction in optical soliton communication systems," *Opt. Lett.* **11**,174-176 (1986)
4. L. F. Mollenauer and J. P. Gordon, *Solitons in Optical Fibers* (Academic, 2006).
5. U. al Khawaja and H. T. C. Stoof, "Formation of matter-wave soliton molecules," *New J. Phys.* **13**, 085003 (2011).
6. M. Stratmann, T. Pagel and F. Mitschke, "Experimental Observation of Temporal Soliton Molecules," *Phys. Rev. Lett.* **95**,143902 (2005).
7. A. Hause, H. Hartwig, B. Seifert, H. Stolz, M. Böhm, and F. Mitschke, "Phase structure of soliton molecules," *Phys. Rev. A* **75**, 063836 (2007).
8. A. Hause, H. Hartwig, M. Böhm, and F. Mitschke, "Binding mechanism of temporal soliton molecules," *Phys. Rev. A* **78**,063815 (2008).
9. R. Nath, P. Pedri, and L. Santos, "Soliton-soliton scattering in dipolar Bose-Einstein condensates," *Phys. Rev. A* **76**, 013606 (2007).
10. B.B. Baizakov, S. M. Al-Marzoug, H. Bahlouli, "Interaction of solitons in one-dimensional dipolar Bose-Einstein condensates and formation of soliton molecules," *Phys. Rev. A* **92**,033605 (2015).
11. K. E. Strecker, Guthrie B. Partridge, Andrew G. Truscott and Randall G. Hule, "Formation and propagation of matter-wave soliton trains," *Nature* **417**,150-153 (2002).
12. L. Khaykovich, F. Schreck, G. Ferrari, T. Bourdel, J. Cubizolles, L. D. Carr, Y. Castin and C. Salomon, "Formation of a Matter-Wave Bright Soliton," *Science* **296**, 1290-1293 (2002).
13. Simon L. Cornish, Sarah T. Thompson, and Carl E. Wieman, "Formation of Bright Matter-Wave Solitons during the Collapse of Attractive Bose-Einstein Condensates," *Phys. Rev. Lett.* **96**,170401 (2006).
14. U. Al Khawaja, H. T. C. Stoof, R. G. Hulet, K. E. Strecker, and G. B. Partridge, "Bright Soliton Trains of Trapped Bose-Einstein Condensates," *Phys. Rev. Lett.* **89**, 200404 (2002).
15. Y. V. Kartashov, B. A. Malomed, and L. Torner, "Solitons in nonlinear lattices," *Rev. Mod. Phys.* **83**, 247 (2011); Erratum *Rev. Mod. Phys.* **83**, 405 (2011).
16. P. G. Kevrekidis, K. Ø. Rasmussen, and A. R. Bishop, "The Discrete Nonlinear Schrödinger Equation: A Survey of Recent Results," *Int. J. Mod. Phys. B* **15**,2833-2900 (2001).

17. T. Kapitula, P. G. Kevrekidis, and B. A. Malomed, "Stability of multiple pulses in discrete systems," *Phys. Rev. E* **63**, 036604 (2001).
18. C. Mejía-Cortés, R. A. Vicencio, and B. A. Malomed, "Mobility of solitons in one-dimensional lattices with the cubic–quintic nonlinearity," *Phys. Rev. E* **88**, 052901 (2013).
19. A. B. Aceves *et al.*, "Discrete self-trapping, soliton interactions, and beam steering in nonlinear waveguide arrays," *Phys. Rev. E* **53**, 1172 (1996).
20. R. Carretero-González, J. D. Talley, C. Chong, B. A. Malomed, "Multistable solitons in the cubic–quintic discrete nonlinear Schrödinger equation," *Physica D* **216**, 77–89 (2006).
21. I. E. Papacharalampous, P. G. Kevrekidis, B. A. Malomed, and D. J. Frantzeskakis, "Soliton collisions in the discrete nonlinear Schrödinger equation," *Phys. Rev. E* **68**, 046604 (2003).
22. Y. S. Kivshar and B. A. Malomed, "Dynamics of solitons in nearly integrable systems," *Rev. Mod. Phys.* **61**, **763** (1989).
23. Y. S. Kivshar and D. K. Campbell, "Peierls-Nabarro potential barrier for highly localized nonlinear modes," *Phys. Rev. E* **48**, 3077–3081 (1993).
24. L. Brizhik, A. Eremko, L. Cruzeiro-Hansson, and Y. Olkhovska, "Soliton dynamics and Peierls-Nabarro barrier in a discrete molecular chain," *Phys. Rev. B* **61**, 1129 (2000).
25. P. G. Kevrekidis, I. G. Kevrekidis, A. R. Bishop, and E. S. Titi, "Continuum approach to discreteness," *Phys. Rev. E* **65**, 046613 (2002).
26. U. Peschel, R. Morandotti, J. M. Arnold, J. S. Aitchison, H. S. Eisenberg, Y. Silberberg, T. Pertsch, and F. Lederer, "Optical discrete solitons in waveguide arrays. 2. Dynamic properties," *J. Opt. Soc. Am. B* **19**, 2637–2644 (2002).
27. H. S. Eisenberg, R. Morandotti, Y. Silberberg, J. M. Arnold, G. Pennelli, and J.S. Aitchison, "Optical discrete solitons in waveguide arrays. I. Soliton formation," *J. Opt. Soc. Am. B* **19**, 2938–2944 (2002).
28. H. He and P. D. Drummond, "Theory of multidimensional parametric band-gap solitons," *Phys. Rev. E* **58**, 5025–5046 (1998).
29. B. Malomed and M. I. Weinstein, "Soliton dynamics in the discrete nonlinear Schrödinger equation," *Phys. Lett. A* **220**, 91–96 (1996).
30. B. A. Malomed, in: *Progress in Optics* **43**, 71–194 (ed. by E. Wolf: North Holland, 2002).
31. P. G. Kevrekidis *The Discrete Nonlinear Schrödinger Equation Mathematical Analysis, Numerical Computations and Physical Perspectives* (Springer, 2009).
32. Y. S. Kivshar and D. K. Campbell, "Peierls-Nabarro potential barrier for highly localized nonlinear modes," *Phys. Rev. E* **48**, 3077 (1993).
33. D. J. Kaup, "Variational solutions for the discrete nonlinear Schrödinger equation," *Mathematics and computers in simulation* **69**, 322–333 (2005).
34. See J. Cuevas and B. A. Malomed in Ref. [31].

1. Introduction

Interaction forces between solitons have been extensively studied in the continuum regime [1–3] as they cause data transfer errors in optical fibres [4]. It is well-established that, at large separations, the force between two solitons decays exponentially with their separation and is proportional to the cosine of their phase difference which was first found by Gordon [2]. The complete form of the potential was then found to be a Morse potential type [5]. Stable soliton molecules were shown to exist in dispersion-managed optical fibres [6–8]. In matter-wave condensates with dipolar interactions, it is believed that real binding between solitons can make a soliton molecule [9, 10]. Bright soliton trains were observed in attractive Bose-Einstein condensates [11–13] followed by a variational calculation that accounted for the repulsive force between the out-of-phase solitons [14].

Discrete solitons, such as optical solitons in waveguide arrays or matter-wave bright solitons of a Bose-Einstein condensation in an optical lattice, show distinctive features in comparison with their continuum counterparts [15, 16], such as multiple pulses binding [17], mobility threshold [18], discrete self-trapping [19], bistability [20], collisions [20, 21], and the presence of the so-called Peierls-Nabarro (PN) effective potential [22–25]. The PN potential is an oscillatory potential with minima located at the waveguides and maxima located between waveguides. The former case corresponds to a stable on-site soliton while the latter corresponds to the unstable inter-site soliton. Existence of stationary solitons, their mobility, and interaction have been well-studied [15, 16, 26, 27]. A general approach for deriving effective potentials of interaction between solitons was presented in [28]. The discrete nonlinear Schrödinger equation, was solved

using variational, perturbative, and numerical approaches [29–31]. Specifically, the height of the PN potential for highly localised nonlinear modes was calculated in Ref. [32] and the two on-site and inter-site stationary states were obtained in Ref. [33]. The profile of the PN potential has been obtained in Refs. [32, 34].

Interactions between discrete solitons in a waveguide array are expected to exhibit some unique features arising from the interplay between the soliton-soliton interaction on one hand, and the solitons interaction with the waveguides on the other hand. It is well-known, for instance, that the mobility of a single soliton will be significantly reduced at high speeds by the PN potential. The essential question we address here is how the soliton-soliton interaction potential will be affected by the presence of the PN potential. Specifically, we aim at obtaining an analytic formula that gives this potential in much the same manner as Gordon's formula describes the interaction between solitons in the continuous case. To that end, we employ a variational calculation with a gaussian trial function which facilitates obtaining compact analytic results. Other trial functions, such as the kusp-like [33] or the hyperbolic secant functions cannot lead to analytic formula for the potential. The theoretical formula we derive here will be compared with the exact interaction potential calculated numerically where good agreement is obtained. In both cases, the significant feature we obtain is the modulation of the oscillatory PN potential to the decaying tail of the interaction potential at large solitons' separation. This leads to the important result of discrete spontaneous soliton molecule formation. In the continuum case, two stationary solitons with a finite separation may spontaneously attract and form a soliton molecule. In the present case, discrete solitons form a molecule only for specific separations. While the solitons form a molecule for odd integer initial soliton separation, they do not so for even integer separation.

Finally, the effect of the soliton-soliton and soliton-waveguide interactions on their dynamics is investigated.

The rest of the paper is organised as follows. In Section 2, we perform the static variational calculation, estimate the two solitons interaction potential, and then compare our results with the potential obtained numerically. In Sec. 3 we discuss the formation of a two solitons molecule. In Sec. 4, we perform a time-dependent variational calculation to study the dynamics of the two solitons. We end up in Section 5 by summarising our main results.

2. Interaction potential

2.1. Variational approach

Our approach in obtaining the interaction potential is to derive the equation of motion for the separation between solitons. The force of interaction, which is the second temporal derivative of the solitons separation, can then be calculated and integrated (summed) to obtain the potential.

The dynamics of discrete solitons is described by the discrete nonlinear Schrödinger equation (DNLSE)

$$i \frac{\partial}{\partial t} \psi_n + d(\psi_{n+1} + \psi_{n-1} - 2\psi_n) + \gamma |\psi_n|^2 \psi_n = 0, \quad (1)$$

where ψ_n is the field amplitude at the n -th lattice site, d and γ are positive strengths of the dispersion and nonlinearity, respectively. The lagrangian corresponding to this DNLSE is given by

$$L = \sum_{n=-\infty}^{\infty} \left[\frac{i}{2} (\psi_n^* \dot{\psi}_n - \dot{\psi}_n \psi_n^*) + d \psi_n^* (\psi_{n+1} + \psi_{n-1} - 2\psi_n) + \frac{\gamma}{2} |\psi_n|^4 \right], \quad (2)$$

where the last two terms define the energy functional

$$E = - \sum_{n=-\infty}^{\infty} \left[d \psi_n^* (\psi_{n+1} + \psi_{n-1} - 2\psi_n) + \frac{\gamma}{2} |\psi_n|^4 \right], \quad (3)$$

and $\dot{\psi}_n$ denotes the derivative of ψ_n with respect to time.

For the static properties, a trial function with minimal number of variational parameters will be adequate, namely the two solitons separation, Δn , and their phase difference $\Delta\phi$. Thus, our trial function for the two solitons, takes the form

$$\psi_n = A e^{-\frac{(n-n_1)^2}{\eta^2} + i\phi_1} + A e^{-\frac{(n-n_2)^2}{\eta^2} + i\phi_2}, \quad (4)$$

where the centres of the two solitons n_1 and n_2 define the separation $\Delta n = n_1 - n_2$ and similarly, the phase difference is defined as $\Delta\phi = \phi_1 - \phi_2$. Clearly, our trial function is simplified by setting the two solitons to have the same amplitude, with no centre-of-mass speeds, and without width breathing and chirp. This situation corresponds to two stationary equal solitons with initially zero relative speed.

For stationary equal amplitude solitons, the centre of mass is always at the mid point between the solitons. Expressions below will be simplified in the frame of reference centered at the midpoint, namely, $n_1 + n_2 = 0$. Normalizing the total power P (or number of atoms in the context of matter-wave solitons)

$$P = \sum_{n=-\infty}^{\infty} \psi_n^* \psi_n \quad (5)$$

we obtain the solitons amplitude in terms of their width

$$A = \frac{\sqrt{P}}{\sqrt{\sqrt{2\pi} \eta \left[\vartheta_3(\Delta n \pi/2, q) + \vartheta_3(0, q) \exp\left(-\frac{(\Delta n)^2}{2\eta^2}\right) \cos(\Delta\phi) \right]}}, \quad (6)$$

where $q = \exp(-\pi^2 \eta^2/2)$ and $\vartheta_3(z, q)$ is the Jacobi theta function defined by $\vartheta_3(z, q) = \sum_{n=-\infty}^{\infty} q^{n^2} e^{2inz}$. The potential of interaction between the two solitons, which equals the energy functional (apart from a pre-factor that can be set to unity, as explained in Sec. 4) is then calculated as

$$V = -d E_K - \frac{\gamma}{2} E_I, \quad (7)$$

where

$$E_K = 4A^2 \sqrt{\frac{\pi}{2}} \eta \left[\vartheta_3(-\pi(\Delta n - 1)/2, q) \exp\left(\frac{-1}{2\eta^2}\right) - \vartheta_3(\pi \Delta n/2, q) + \left(\vartheta_3(\pi/2, q) \exp\left(\frac{-1}{2\eta^2}\right) \cosh\left(\frac{\Delta n}{\eta^2}\right) - \vartheta_3(0, q) \right) \exp\left(-\frac{(\Delta n)^2}{2\eta^2}\right) \cos(\Delta\phi) \right], \quad (8)$$

$$E_I = A^4 \sqrt{\pi} \eta \left[\vartheta_3(\pi \Delta n/2, \sqrt{q}) + \vartheta_3(0, \sqrt{q}) \exp\left(\frac{-(\Delta n)^2}{\eta^2}\right) (2 + \cos(2\Delta\phi)) + 4\vartheta_3(\pi \Delta n/4, \sqrt{q}) \exp\left(\frac{-3(\Delta n)^2}{4\eta^2}\right) \cos(\Delta\phi) \right]. \quad (9)$$

Since the soliton typically extends over several waveguides, i.e., $\eta > 1$, the quantity $q = \exp(-\pi^2 \eta^2/2)$, which is the argument of the Jacobi function, will be much less than one. In this case, we can simplify the energy functional by expanding in q around zero, leading to

$$V[\Delta n, \Delta\phi(\Delta n)] = V_0 + \frac{P}{4\sqrt{\pi}\eta} \left[P\gamma + 8\sqrt{\pi}\eta y d \left(1 - \cosh(\Delta n/\eta^2) \right) \right] \exp\left(-\frac{(\Delta n)^2}{2\eta^2}\right) \cos \Delta\phi + P \left(8dy + \frac{P\gamma}{\sqrt{\pi}\eta} \right) q \cos(\pi \Delta n) \quad (10)$$

where we have defined the noninteracting solitons energy as

$$V_0 = 2Pd(1 - y) - \frac{P^2\gamma}{4\sqrt{\pi}\eta} \quad (11)$$

and $y = \exp(-1/2\eta^2)$. Interestingly, the interaction between solitons given by Eq. (10) is the sum of a molecular type soliton-soliton interaction (zeroth order term) and their interaction with the waveguide (the first order term) characterised by an oscillatory dependence on solitons separation. In fact, this corresponds to the Pierls-Nabarro potential of the two solitons. Being a first order contribution, the oscillatory part will have a noticeable effect only near the tail region of the potential. Another interesting feature of the oscillatory contribution is its dependence on whether solitons separation Δn is an even integer, odd integer, or a half integer. For the integer case, both solitons are either at the minima or the maxima of the PN potential. If both are at the minima, the two solitons will be stable against centre of mass perturbations preventing spontaneous solitons binding unless they are too close such that their zeroth order interaction overcomes this small PN barrier. For the even integer case, both solitons are located initially at the maxima of the PN potential. They will be unstable and both solitons will eventually fall to the next minimum of the PN potential, which takes us back to the odd integer case. The situation is very different when Δn is half integer, which corresponds to one of the solitons being at the minimum of the PN potential, while the other is at the maximum. While the former is stable, the latter is not. Any small perturbation will cause the latter soliton to move which changes the solitons separation and leads to spontaneous binding. The sensitivity of spontaneous binding to discreteness is a unique feature of solitons interacting in a waveguide array and is not present in the continuum case. In Sec. 2.2, this behavior will be confirmed numerically.

The phase difference between solitons changes while the solitons approach each other. To find how $\Delta\phi$ depends on solitons separation, we ought to perform a time-dependent variational calculation where equations of motion for $\Delta n(t)$ and $\Delta\phi(t)$ will be derived from their equations of motion. Time will then be eliminated in order to obtain $\Delta\phi(\Delta n)$. As a rough approximation, a constant phase difference may be set for, say in-phase solitons, $\Delta\phi = 0$, or out-of-phase solitons, $\Delta\phi = \pi$. For the in-phase option, the solitons will have their minimum energy for zero separation, which means that no molecular type binding will take place. For the out-of-phase case, a repulsive part exists in the energy functional giving rise to a molecular type potential with a finite bond length. However, when compared with the exact numerical solution, the bond length and energy will be very different from the exact ones. In reality, the situation is none of these two simple cases; the phase difference changes with their separation and we need to include that dependence in order to account for the exact potential, at least within a reasonable approximation. Performing the time-dependent variational calculation will not be helpful for this purpose due to the complicated equations of motion that do not allow for obtaining analytical solutions for $\Delta n(t)$ and $\Delta\phi(t)$, let alone the yet harder problem of eliminating time between them. Our approach for finding $\Delta\phi(\Delta n)$ will be guided by the numerical solution described in the next section. Specifically, we will show that $\Delta\phi(\Delta n)$ behaves as Δn^{-4} for Δn around the potential well. For larger separations, $\Delta\phi$ decays exponentially as $\exp(-\Delta n/\eta)$. The former behavior is responsible for obtaining the correct molecular part of the potential around the equilibrium bond length with good estimates for the bond length and strength. The latter, has a negligible contribution in the region near the equilibrium bond length. Besides, it should be noted that the $\cos \Delta\phi$ term appearing in the potential, (10), multiplied by either $\exp(-(\Delta n)^2/2\eta^2)$ or $q = \exp(-\pi^2\eta^2/2)$, both of which are very small in the tail region. Thus, consistent with the first order expansion in (10), we may take

$$\Delta\phi(\Delta n) = \frac{c}{\Delta n^4}, \quad (12)$$

where c is a constant to be determined from the boundary condition on $\Delta\phi(\Delta n_f)$, Δn_f is the

shortest bond length as will be shown in the next section.

Finally, the equilibrium soliton width, η_{eq} , is accurately calculated by minimizing the energy functional of a single soliton with respect to η , namely $\partial E_s / \partial \eta |_{\eta_{eq}} = 0$, where E_s is the energy of a single soliton, given by $E_s = V_0(P/2)$. We divide P by 2 since V_0 corresponds to the energy of two infinitely separated solitons.

2.2. Numerical calculation

Here, we use the alternative approach to find the interaction potential between two solitons by calculating numerically the solitons separation, from which the force and potential of interaction are determined. At first, we calculate the stationary profile of the two solitons for a given initial separation. The Newton-Raphson method is used, and the result for one specific case is shown in Fig. 1. We plot also in this figure the variational trial function, (4), for the same parameters, to see that it makes a good representation of the exact solution. It is of course known that the gaussian function does not describe accurately the tail which decays exponentially. For solitons extending over several waveguides, the gaussian represents accurately the exact profile, but for narrow solitons, obtained with small γ or large d , the gaussian is not a good representation of the exact solution especially in the tail and overlap regions.

Having found the stationary profile, we evolve it in time by solving the time-dependent DNLS, Eq. (1). The two solitons attract and approach each other until they coalesce, then they repel but come back and coalesce again and so on, as shown in Fig. 1. This is very similar to the continuum case, but with some significant differences that will be pointed out in the next section. Calculating numerically the solitons separation $\Delta n(t)$, then differentiating twice to get the force between the two solitons

$$F = \frac{d^2}{dt^2} \Delta n(t) \quad (13)$$

the potential is then obtained by integrating the force with respect to $\Delta n(t)$

$$V = - \int_{\Delta n_i}^{\Delta n_f} F(\Delta n) d(\Delta n). \quad (14)$$

The limits of the integration range from the initial arbitrary separation Δn_i to the shortest final separation Δn_f . Larger values of Δn_i are desirable since they will allow for a determination of the tail of the potential for large separations. However, for too large initial solitons separation, they may not bind due to the weakness of their interaction and the presence of the PN potential. The final solitons separation Δn_f can not be less than the solitons shortest approach separation which is of the order of one soliton width, namely η_{eq} . Numerically, we run the time evolution code until the two solitons reach their first coalescence. This will give the potential in the region $[\Delta n_i, \Delta n_f]$. In Fig. 2, we show the force, potential, and phase difference curves. Interestingly, the small PN potential oscillatory part of the potential is clearly visible in the tail of the otherwise molecular type potential.

An important feature that Fig. 2 shows is the dependence of the phase difference on solitons separation. Attempting to find this functional behaviour, we considered three cases with different initial separations. We had to change the strength of the nonlinear interaction for each case such that the soliton width is large enough to allow for an overlap and interaction. We plot in Fig. 3 the phase difference curves versus the solitons separation on a log-log and semi-log plots. The log-log plots show that for most of the solitons separation range, the behaviour is non-polynomial, except near the shortest separation region where the curves are linear with slope equal to -4 . The semi-log curves show that the behaviour is in fact exponential for most of the range, except near short separations. To confirm that the behaviour for short separations is not exponential, we plot also $\Delta \phi \times (\Delta n)^4$ versus Δn to see that indeed for the range between $\Delta n \approx 2.5$ and $\Delta n \approx 5.5$ the curves are almost constant on the average and start decaying beyond

$\Delta n \approx 5.5$ where the exponential decay starts to dominate. As discussed in the previous section, the Δn^{-4} behaviour takes place in the important region of the potential, namely its minimum where the bond length and strength will be determined. For this reason we approximate the functional dependence of the phase separation by the Δn^{-4} law, as given by Eq. (12). The numerical curves of the phase difference show that at the phase difference between the two solitons at their shortest separation equals $\pi/2$. The proportionality constant, c , is thus determined from the boundary condition $\Delta\phi(\eta_f) = \pi/2$. We estimate the shortest separation, η_f , by the single soliton width, η_0 , since the two solitons merge at the coalescence point. Therefore, the constant c is determined by

$$\frac{c}{\eta_{\text{eq}}^4} = \frac{\pi}{2}. \quad (15)$$

Since η_{eq} is obtained from the single soliton energy, the only input that the numerical calculation supplies to the variational one is the $\pi/2$ value at the shortest separation. Calculating c for the three cases considered, we plot in Fig. 3 the power law $c/(\Delta n)^4$ together with the corresponding numerical curves which show excellent agreement especially in the short separation region, as expected.

Finally, we use the power law for the phase difference dependence on separation in the interaction potential formula, (10), and compare the resulting potential curve with the numerical one, as shown in Fig. 4. Qualitative agreement is obtained with a molecular type of potential. As discussed previously, there is no significant effect of not taking into account the exponential decay of the phase difference. This is evident from the very good agreement between the theoretical and numerical curves in the tail region. The agreement on the bond length and strength can be enhanced by considering the full energy functional given by Eqs. (7-9). Figure 4 shows that the full variational approach captures most of the features of the exact numerical potential. The oscillating tail, which is clearly visible in the numerical curve, is present in the theoretical one but with much less amplitude due to the fact that the gaussian ansatz is not accurate in the tail region, as shown in Fig. 5. It decays much faster than the exponential, hence the suppression of the amplitude of the PN oscillations.

The essential feature that the PN potential introduces is the discreteness in the spontaneous soliton molecule formation. This is shown in Fig. 6 where spontaneous solitons binding does not necessarily always occur for shorter solitons separations. While the solitons bind for $\Delta n_i = 13$, they do not bind for $\Delta n_i = 10$. Since we took the centre of our frame of reference between the two solitons such that $n_1 + n_2 = 0$, the first initial solitons separation $\Delta n_i = 13$ corresponds to $n_1 = 6.5$ and $n_2 = -6.5$. However, in Fig. 6, we shift the centre of mass of the two solitons to the middle of the waveguide array, which is an integer value of 60. Thus the solitons in this case are initially entered at 66.5 and 53.5. Solitons at the intersites are unstable, therefore the two solitons in this case were able to bind. In the case of shorter initial separation, $\Delta n_i = 12$, the two solitons are on-site at 66 and 54. The PN potential is minimum there preventing the two solitons from binding.

3. Solitons binding

In this section, we discuss the possibility that the interaction between two solitons bind them in a molecule-like structure. This problem has been considered by Ref. [17] focusing on the stability of the bound states. Here, we have a different focus, which is the effect of the PN potential on the spontaneous formation of the bound state. We have shown in previous sections that the interaction potential between discrete solitons is indeed of a molecular type. Thus, solitons binding is anticipated. However, it is well-known in the continuum case that the binding energy between solitons is zero, which means that the bond is highly unstable against perturbations [29,30]. The situation for discrete solitons is similar with the exception of a certain region in the parameter space where the PN potential can stabilise the bond. Stabilising the, otherwise fragile,

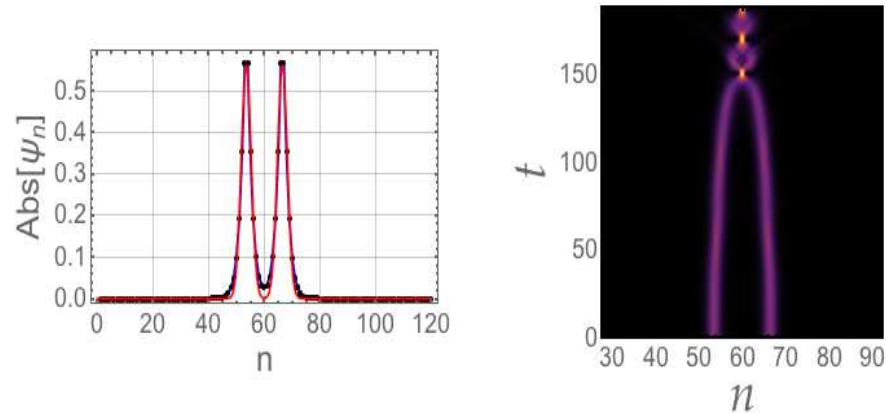


Fig. 1. Left: Initial stationary two solitons' profile as obtained by numerical solution of the DNLSE, Eq. (1), (black lines with dots) and the variational trial function (red line). Right: Spacio-temporal density plot of the evolution of the initial state on the left panel. The parameters used are: $\gamma = 1$, $d = 0.38$, initial separation $\Delta n(0) = 13$, $P = 2$

bond between the solitons is known in dispersion-managed fibers [6] and dipolar condensates [9], where a *true* bond between the solitons exists to form a *true* soliton molecule.

There are two distinct regimes for the interaction between discrete solitons. The first is a continuum-like where the width of the solitons is considerably larger than the separation between waveguides. In this case, the discrete nature of the solitons is almost absent and, as mentioned above, the binding between solitons is fragile since any small perturbation can break the bond. The second regime is when the solitons width is comparable to just few waveguides. For the discreteness of the soliton to have tangible effect and for the PN potential to have a significant role, the separation between the two solitons should be large enough so that the strength of the interaction between solitons be of the order of the PN potential. Therefore, one needs to search in the three parameters space: strength of nonlinearity, γ , dispersion, d , and solitons initial separation, $\Delta n(0)$. Large γ or small d take the solitons deeper in the discrete regime which leads to higher PN potential. The initial separation controls the strength of the interaction between solitons. Inspection of these parameters leads us to find a regime where the PN potential results in real binding between the solitons. In the following we present the evidence for the latter through several numerical experiments. In Fig. 7, we plot the separation of two solitons located initially at the minima of the PN potential (integer values of solitons centres). Clearly, the solitons initially attract each other but then repel due to the presence of the PN barrier between them. While this shows that the solitons indeed interact, it may not be an evidence that they are bound to each other, i.e., the solitons may separate once one of them is given a kick. To test this possibility, we have given a velocity kick to only one of the solitons and looked for a situation where the other one followed. Indeed this is what we find in Fig. 8, where the soliton on the right was initially kicked. Clearly the soliton on the left followed. However, the velocity kick should not be too large since otherwise there will be not enough time for the left soliton to respond. The key feature in this figure is that the two solitons move for a considerable time over many waveguides overcoming many PN potential maxima, which proves that it is a real binding and real molecule. Due to the pinning nature of solitons flowing in waveguide arrays the solitons speed decrease to reach the critical mobility speed at which the solitons will be pinned either separately or after being coalesced.

Coalescence of solitons is known in the continuum case, however, solitons then split again.

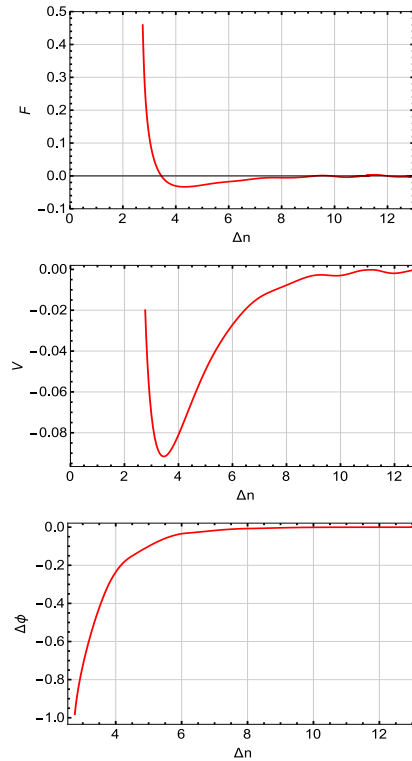


Fig. 2. Force (upper), potential (middle), and phase difference (lower panel) between the two solitons considered in Fig. 1.

Discrete solitons may also do the same, as seen for instance in Fig. 1, but for certain values of the parameters, the solitons may be pinned by one waveguide after coalescence, as shown in Fig. 9. This feature may be useful for applications of waveguide arrays in performing logic operations. Specifically, the process in Fig. 9 represents an AND gate where the two inputs correspond to the two initial solitons and the output is taken from the waveguide at their middle. The output will be 1 only when both solitons are present, and will be zero otherwise.

4. Equations of motion and dynamics

In this section we use a time-dependent variational calculation to derive the equations of motion for the two interacting solitons. It is aimed at obtaining further insight into the mechanism of binding as well as the peculiarities in their dynamics resulting from discreteness.

Unlike the static variational calculation in Sec. 2.1, we need here to include the two additional degrees of freedom of the center of mass motion and breathing. It is important to include breathing, which requires the inclusion of chirp, in order to account for the repulsion at short separations, since otherwise the two solitons will always coalesce. The trial function takes the form

$$\psi_n = A e^{-\frac{(n-n_1(t))^2}{\eta(t)^2} + ik_1(t)(n-n_1(t)) + i\beta(t)(n-n_1(t))^2 + i\phi_1(t)} + A e^{-\frac{(n-n_2(t))^2}{\eta(t)^2} + ik_2(t)(n-n_2(t)) + i\beta(t)(n-n_2(t))^2 + i\phi_2(t)}. \quad (16)$$

It is instructive to define the variational parameters of the single solitons in terms of their relative and centre of mass analogues, as follows:

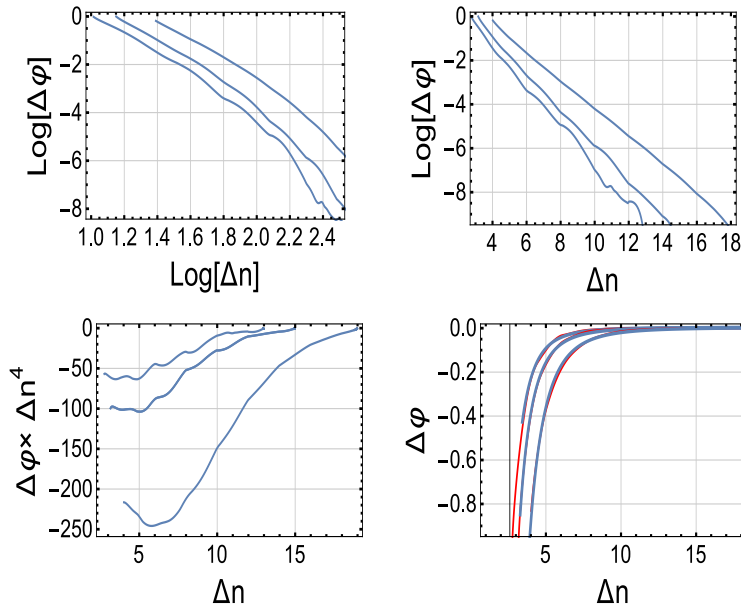


Fig. 3. Phase difference between two solitons for three different values of initial separation and nonlinearity strength. The parameters for the lowest curve are: $\Delta n_i = 13$, $\gamma = 1$, for the middle curve: $\Delta n_i = 15$, $\gamma = 0.9$, and for the upper curve: $\Delta n_i = 19$, $\gamma = 0.7$. For all curves: $d = 0.38$ and $P = 2$. Blue lines correspond to the numerical calculation and the red lines correspond to the power law fit $\Delta\phi = c/(\Delta n)^4$, where c for each curve was determined by the condition (15).

$$\begin{aligned}
 n_0(t) &= n_1(t) + n_2(t), & \Delta n(t) &= n_1(t) - n_2(t), \\
 k_0(t) &= k_1(t) + k_2(t), & \Delta k(t) &= k_1(t) - k_2(t), \\
 \phi_0(t) &= \phi_1(t) + \phi_2(t), & \Delta\phi(t) &= \phi_1(t) - \phi_2(t),
 \end{aligned} \tag{17}$$

Calculating the lagrangian given by Eq. (2) using this trial function, we obtain

$$L = \frac{P}{4} \left[(k_0 \dot{n}_0 + \Delta k \Delta \dot{n} - \eta^2 \dot{\beta} - 2\dot{\phi}_0) \right] - V. \tag{18}$$

Here V is the generalization of the soliton-soliton interaction potential, Eq. (10), to the case with center of mass momentum, k_0 , relative momentum, Δk , breathing, η , and chirp, β , namely

$$V = V_{ss} + V_{sw} \tag{19}$$

where we have decomposed the interaction potential into a soliton-soliton part

$$V_{ss} = V_0[k_0, \Delta k, \beta, \eta] + \frac{P}{4\sqrt{\pi}\eta} \left[P\gamma + 8\sqrt{\pi} d \eta \exp\left(-\frac{1}{2\eta^2}\right) \left(1 - \cosh\left(\frac{\Delta n}{\eta^2}\right)\right) \right] \exp\left(-\frac{(\Delta n)^2}{2\eta^2}\right) \cos \Delta\phi \tag{20}$$

and a soliton-waveguide part

$$V_{sw} = P \left[8d \exp\left(-\frac{1}{2\eta^2}\right) + \frac{P\gamma}{\sqrt{\pi}\eta} \right] \exp\left(-\frac{\pi^2 \eta^2}{2}\right) \cos(\pi \Delta n) \cos(\pi n_0), \tag{21}$$

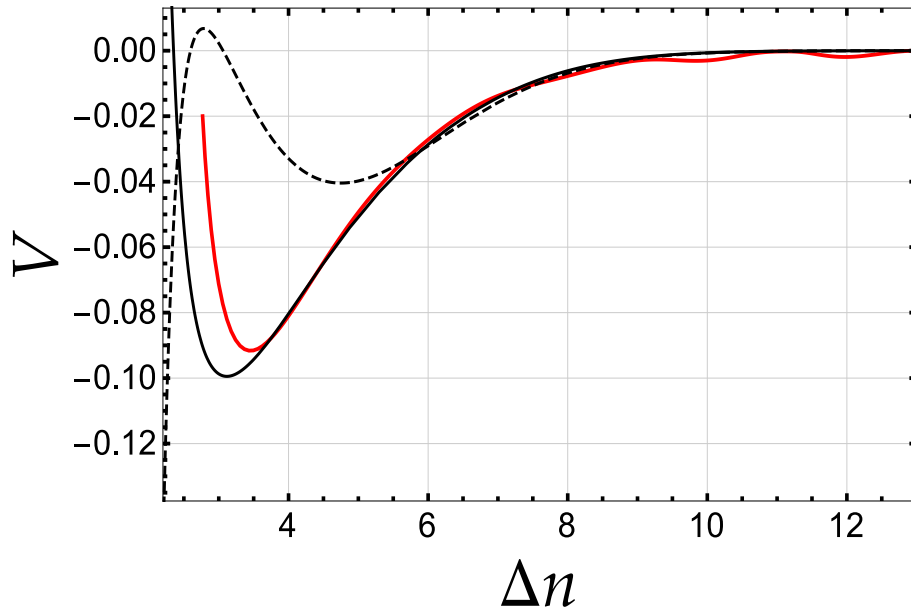


Fig. 4. Interaction potential between two discrete solitons. Black solid curve corresponds to the full variational calculation, Eq. (7), dashed curve corresponds to the approximate formula Eq. (10), and the red curve corresponds to the numerical solution. Parameters used are: $\gamma = 1$, $d = 0.5$, $P = 2$.

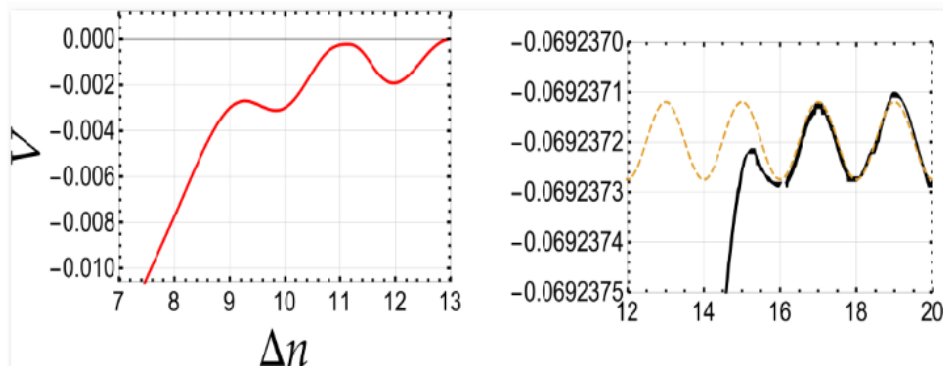


Fig. 5. Zoom-in of Fig. 4 in the tail region. Red dashed curve corresponds to the PN potential.

with

$$V_0 = 2Pd \left[1 - \exp\left(-\frac{1}{2\eta^2}\right) \cos\left(\frac{k_0}{2}\right) \cos\left(\frac{\Delta k}{2}\right) \right] - \frac{P^2\gamma}{4\sqrt{\pi}\eta}, \quad (22)$$

and we have assumed the limit $\Delta n \gg \eta$. It should be noted that Eq. (19) is identical to Eq. (10), apart from the new definition of V_0 , as given now by Eq. (22).

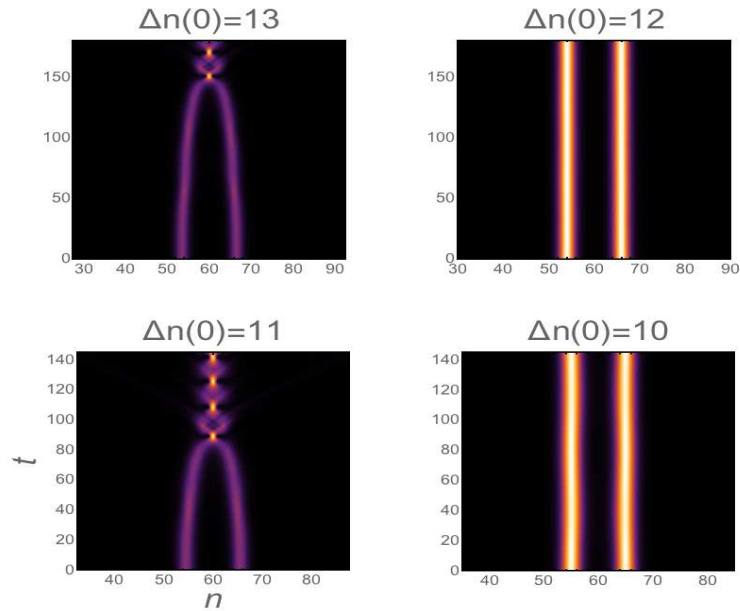


Fig. 6. Spatio-temporal density plots showing the two solitons time evolution for different initial separations. Parameters used are: $\gamma = 1$, $d = 0.38$, $P = 2$.

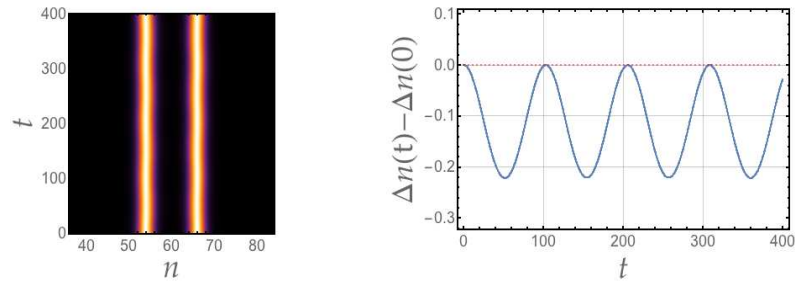


Fig. 7. Two solitons located initially at the minima of the PN potential ($n_1 = 54$, $n_2 = 66$). We have used $\gamma = 1.0$, $d = 0.4$.

4.1. Equations of motion

Insight into the solitons interaction and dynamics can be obtained from the reduced equations of motion where large soliton widths and separation are considered. Soliton width should not be considerably larger than unity in order to be in this limit. Terms containing $\exp(-\pi^2\eta(t)^2/2)$ are already much smaller than unity for $\eta(t)$ of order unity. Terms containing $\exp(-\Delta n(t)^2\eta(t)^2/2)$ are also very small for values of $\Delta n(t)$ just several times larger than $\eta(t)$. Within these limits, the equations of motion simplify to

$$\dot{n}_0 = 2d \exp\left(-\frac{\pi^2\eta^2}{2}\right) \cos\left(\frac{\Delta k}{2}\right) \sin\left(\frac{k_0}{2}\right), \quad (23)$$

$$\Delta \dot{n} = 2d \exp\left(-\frac{\eta^2\beta^2}{2}\right) \sin\left(\frac{\Delta k}{2}\right) \cos\left(\frac{k_0}{2}\right), \quad (24)$$

$$\dot{k}_0 = -\frac{4}{P} \frac{dV_{sw}}{dn_0}, \quad (25)$$

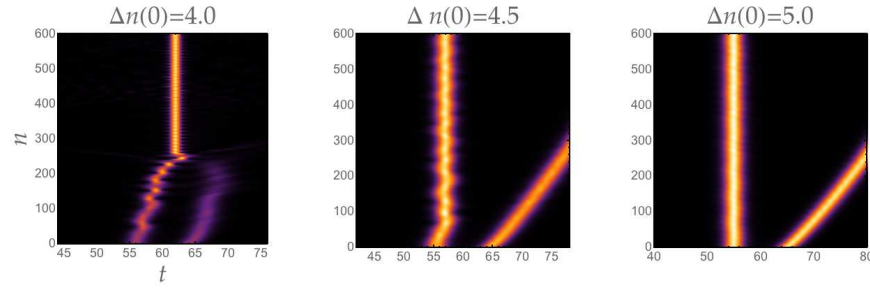


Fig. 8. Two solitons located at different initial separations and the right soliton in each subfigure was given an initial velocity kick of 0.115. We have used $\gamma = 1.0$, $d = 0.4$.

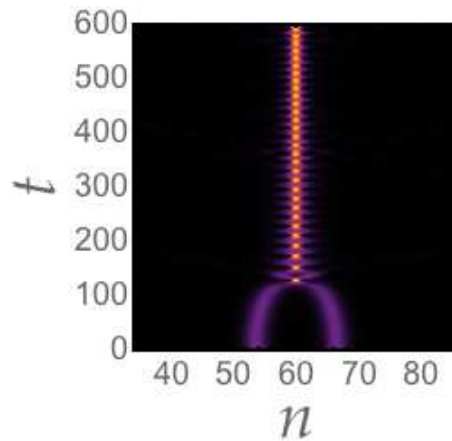


Fig. 9. Two solitons located initially at the maxima of the PN potential ($n_1 = 53.5$, $n_2 = 66.5$). $\gamma = 1.0$, $d = 0.4$.

$$\Delta \dot{k} = -\frac{4}{P} \left(\frac{dV_{ss}}{d(\Delta n)} + \frac{dV_{sw}}{d(\Delta n)} \right). \quad (26)$$

Differentiating Eq. (24) with respect to time and using Eqs. (25) and (26), a reduced equation of motion for the solitons separation can be derived, in the limit of small speeds and chirp

$$\Delta \ddot{n} = -\frac{4d}{P} \frac{dV}{d(\Delta n)}. \quad (27)$$

The right hand side of this equation gives the force of interaction between the solitons. Their interaction potential is thus $(4d/P)V$, which according to Eq. (19) is composed of the soliton-soliton and soliton-waveguide interaction potentials. This potential is plotted against the exact numerical one as discussed earlier and shown in Fig. 4. The figure shows that the variational calculation accounts reasonably to the strength and length of the bond between the solitons (depth and location of minimum of the potential well). Note that we selected the parameters of Fig. 4 such that the prefactor $4d/P$ is unity, which means that the interaction potential between solitons $(4d/P)V$, as inferred by Eq. (27), equals the energy functional V given by Eq. (7). There are two distinguished limits where specific solutions can be obtained, namely when the two solitons are close enough such that $V_{ss} \gg V_{sw}$ and separated enough such that $V_{ss} \ll V_{sw}$. In the former case, the dynamics of the separation between solitons is similar to that of a single particle in the potential well of V_{ss} , which can with some simplifications be sinusoidal. The

solutions in this case are oscillatory around zero, which indicates that solitons coalesce, as for instance, in Fig. 1. In the latter case, the solution is oscillatory but around a finite value. Specifically, the equation of motion will take the form

$$\Delta \ddot{n} = c \sin(\pi \Delta n), \quad (28)$$

where $c = 4\pi d \left[8d \exp(-1/(2\eta^2)) + P\gamma/(\sqrt{\pi}\eta) \right] \exp(-\pi^2\eta^2/2)$ and we have assumed, without loss of generality, $n_0(t) = 0$. The solution of Eq. (28) is the Jacobi amplitude function

$$\Delta n(t) = 2 \operatorname{am} \left(\frac{1}{2} \sqrt{c_1 - 2c} (x + c_2)^2, \frac{4c}{2c - c_1} \right), \quad (29)$$

where c_1 and c_2 are two arbitrary constants, determined by the initial conditions. The solitons separation described by this solution remains constant for a while before rather quick transition to a separation that is shorter by two waveguides which corresponds to a hopping of both solitons to the adjacent waveguide between the solitons.

Similarly, an equation for the centre of mass can be derived

$$\ddot{n}_0 = -\frac{4d}{P} \frac{dV_{sw}}{d(\Delta n)}. \quad (30)$$

Substituting V_{sw} from Eq. (21), this equation will have essentially the same solution as (29). This shows, together with Eq. (25), that the centre of mass dynamics is driven only by the soliton-waveguide interaction.

5. Conclusions

We have used the variational approach with a gaussian trial function to obtain the interaction potential between two discrete solitons. The main features of the interaction potential are the co-presence of the soliton-soliton molecular type of interaction together with a periodic part stemming from the interaction between the solitons and the waveguide array, namely the PN potential. The periodic part of the interaction is more visible near the tail region of the potential where it has also the maximum effect on the features of the soliton, as it is the case for example in the spontaneous soliton molecule formation. If the two solitons were initially located with a separation where the PN potential has a noticeable effect, the solitons bind only when their separation is an odd number. This is consistent with the previous knowledge about onsite discrete solitons being stable against centre of mass perturbations while intersite solitons being unstable and become mobile for any perturbation. In the two solitons case, an odd integer separation corresponds to the two solitons being at the intersites (taking their centre of mass to be onsite), and thus unstable. This allows for their soliton-soliton interaction to bind them. For even integer separations, the two solitons are stable and the soliton-soliton interaction has to exceed a finite threshold before being able to bind them. The effects of the PN potential on the soliton-soliton interaction diminish when the two solitons are initially located either too far or too close. In such a case, the interaction potential reduces to its continuum value.

We have used a time-dependent variational calculation to derive the solitons equations of motion. The interaction potential was recalculated from the equation of motion of the solitons separation. Specific solutions in the limit of large separation were also obtained analytically.

It is expected that other unique features related to the mobility of the two solitons and their scattering and interaction with external potentials may exist, their investigation will be left for future work.

Acknowledgment

This project was funded by the National Plan for Science, Technology and Innovation (MAAR-IFAH) - King Abdulaziz City for Science and Technology - through the Science & Technology

Unit at King Fahd University of Petroleum & Minerals (KFUPM) - the Kingdom of Saudi Arabia, award number 14-NAN667-04.